Chinese Journal of Natural Medicines

Nuciferine alleviates collagen-induced arthritic in rats by inhibiting the proliferation and invasion of human arthritis-derived fibroblast-like synoviocytes and rectifying Th17/Treg imbalance

Hao WANG, Xiaolong GENG, Fangbin AI, Zhilun YU, Yan ZHANG, Beibei ZHANG, Cheng LV, Ruiyang GAO, Bei YUE, Wei DOU

Citation: Hao WANG, Xiaolong GENG, Fangbin AI, Zhilun YU, Yan ZHANG, Beibei ZHANG, Cheng LV, Ruiyang GAO, Bei YUE, Wei DOU, Nuciferine alleviates collagen-induced arthritic in rats by inhibiting the proliferation and invasion of human arthritis-derived fibroblast-like synoviocytes and rectifying Th17/Treg imbalance, Chinese Journal of Natural Medicines, 2024, 22(4), 341-355. doi: 10.1016/S1875-5364(24)60622-9.

View online: https://doi.org/10.1016/S1875-5364(24)60622-9

Available online at www.sciencedirect.com
ScienceDirect
Chinese Journal of Natural Medicines 2024, **22**(4): 341-355
doi: 10.1016/S1875-5364(24)60622-9
Chinese Journal of Natural Medicines

•Original article•

Nuciferine alleviates collagen-induced arthritic in rats by inhibiting the proliferation and invasion of human arthritis-derived fibroblast-like synoviocytes and rectifying Th17/Treg imbalance

WANG Hao[Δ], GENG Xiaolong[Δ], AI Fangbin, YU Zhilun, ZHANG Yan, ZHANG Beibei, LV Cheng, GAO Ruiyang, YUE Bei[*], DOU Wei[*]

The MOE Key Laboratory of Standardization of Chinese Medicines, Shanghai Key Laboratory of Compound Chinese Medicines, and the SATCM Key Laboratory of New Resources and Quality Evaluation of Chinese Medicine, Institute of Chinese Materia Medica, School of Traditional Chinese Materia Medica, Shanghai University of Traditional Chinese Medicine (SHUTCM), Shanghai 201203, China

Available online 20 Apr., 2024

[ABSTRACT] Rheumatoid arthritis (RA) is a chronic autoimmune disorder marked by persistent synovial inflammation and joint degradation, posing challenges in the development of effective treatments. Nuciferine, an alkaloid found in lotus leaf, has shown promising anti-inflammatory and anti-tumor effects, yet its efficacy in RA treatment remains unexplored. This study investigated the anti-proliferative effects of nuciferine on the MH7A cell line, a human RA-derived fibroblast-like synoviocyte, revealing its ability to inhibit cell proliferation, promote apoptosis, induce apoptosis, and cause G_1/S phase arrest. Additionally, nuciferine significantly reduced the migration and invasion capabilities of MH7A cells. The therapeutic potential of nuciferine was further evaluated in a collagen-induced arthritis (CIA) rat model, where it markedly alleviated joint swelling, synovial hyperplasia, cartilage injury, and inflammatory infiltration. Nuciferine also improved collagen-induced bone erosion, decreased pro-inflammatory cytokines and serum immunoglobulins (IgG, IgG1, IgG2a), and restored the balance between T helper (Th) 17 and regulatory T cells in the spleen of CIA rats. These results indicate that nuciferine may offer therapeutic advantages for RA by decreasing the proliferation and invasiveness of FLS cells and correcting the Th17/Treg cell imbalance in CIA rats.

[KEY WORDS] Rheumatoid arthritis; Collagen-induced arthritis; Fibroblast-like synoviocyte; Immune imbalance; Nuciferine
[CLC Number] R965 **[Document code]** A **[Article ID]** 2095-6975(2024)04-0341-15

Introduction

Rheumatoid arthritis (RA) is a complex and currently incurable condition that impacts millions globally [1]. It is characterized by synovial hyperplasia, bone erosion, and immune system imbalance, largely due to the abnormal activation of fibroblast-like synoviocytes (FLSs) [2-3]. FLS cells, predominating in the synovial joints, display tumor-like characteristics, including enhanced adhesion and invasion capabilities, coupled with a resistance to apoptosis [4-5]. In the inflammatory environment, FLS cells release various cytokines such as tumor necrosis factor-alpha (TNF-α), interleukin (IL)-6, IL-23, and matrix metalloproteinases (MMPs) [6-7]. These cytokines and MMPs are key contributors to inflammatory pathways, facilitating pannus formation and the breakdown of extracellular matrix components [8].

Accumulating evidence suggests that abnormalities in lymphocytes within the peripheral blood, especially the imbalance in subpopulations of immunocompetent cells such as T helper (Th) 17 and regulatory T (Treg) cells, play a pivotal role in the onset of RA [9]. The sustained infiltration of $CD4^+$ T cells, macrophages, and dendritic cells into the synovial tissue intensifies the activation of FLS cells [10]. Theoretically, naive $CD4^+$ T cells can differentiate into two primary types of effector T cells: Th17 cells and T cells [11]. Th17 cells are known to provoke the inflammatory response and exacerbate synovitis through the production of the pro-inflammatory IL-17. Conversely, T cells aim to regulate the aberrant autoimmune response by secreting the anti-inflammatory IL-10 [12].

[Received on] 28-Jul.-2023
[Research funding] This work was supported by the National Natural Science Foundation of China (No. 82274329, 82304991), the China Postdoctoral Science Foundation (No, 2023M732336), and Shanghai Science and Technology Committee Sailing Program Foundation (No. 23YF1442500).
[*Corresponding author] E-mails: yuebei@shutcm.edu.cn (YUE Bei); douwei@shutcm.edu.cn
[Δ]These authors contributed equally to this work.
These authors have no conflict of interest to declare.

A significant body of research links the pathogenesis of RA to a disruption in the balance between Th17 and T cells [13].

Current clinical approaches for managing RA predominantly include the use of chemical medications, such as conventional synthetic disease-modifying antirheumatic drugs (DMARDs), glucocorticoids, and biologic therapies [1, 14]. Despite their effectiveness, modalities are often accompanied by a range of adverse reactions, including hepatorenal toxicity, increased risk of infections, and potential tumor development. This highlights the critical need for the exploration and development of new therapeutic agents [15].

Nuciferine (chemical structure is shown in Fig. 1A), an aporphine alkaloid predominantly found in *Nelumbo nucifera* leaves—which are utilized in teas and extracts—holds a reputation for promoting weight loss, reducing water retention, eliminating free radicals, delaying aging, and preventing chronic diseases [16]. It exhibits a wide range of pharmacological activities, including stimulation of insulin secretion, mitigation of atherosclerosis, improvement of liver steatosis, and demonstration of anti-tumor and antioxidant properties [17-19]. Prior research has highlighted nuciferine's ability to protect against bone damage by inhibiting the formation of multinucleated osteoclasts and promoting the development of type H vessels [20, 21]. Yet, the specific mechanisms by which nuciferine alleviates bone-related inflammatory responses remain to be fully elucidated. In this study, a collagen-induced arthritis (CIA) rat model was used to explore the therapeutic effects and mechanisms of nuciferine, focusing also on its antiproliferative, anti-invasive, and pro-apoptotic impacts on human RA-derived FLS cells.

Materials and Methods

Cell culture

The MH7A FLS cell line, derived from the synovial tissue of an RA patient, was sourced from Jennio Biotech Co., Ltd. (Guangzhou, China). The cells were cultured in Dulbecco's modified Eagle's medium (DMEM) enriched with 10% fetal bovine serum (FBS) and 1% penicillin/streptomycin., under a humidified atmosphere containing 5% CO_2 at 37 °C. Both the DMEM medium and FBS were procured from Thermo Fisher Scientific (Gibco, Grand Island, NY, USA), while the penicillin/streptomycin was obtained from Sigma (St. Louis, MO, USA).

Cell viability assay

MH7A cells were plated at a density of 5×10^3 cells/well plates and treated with various concentrations of nuciferine (with a purity of > 98%; sourced from Yuanye Bio-Technology, Shanghai, China), including 0, 10, 20, 40, 60, 80, 100, 120, 140, and 160 μmol·L^{-1} for a duration of 48 h. Following treatment, cell viability was assessed using the Cell Counting Kit-8 (CCK-8) assay (Dojindo, Kumamoto, Japan). After incubation with 10% of CCK-8 solution, the absorbance was measured at a wavelength of 450 nm utilizing a spectrophotometer (BioTek, Winooski, VT, USA).

Colony formation assay

To assess the impact of nuciferine on the colony-forming capability of MH7A cells, we employed the transwell assay. Specifically, MH7A cells were plated at a density of 1000 cells/well into the upper chambers of the transwell system and allowed to form colonies. The cells were then treated with varying concentrations of nuciferine (0, 20, 40, and 80 μmol·L^{-1}) over a period of 7 d. After treatment, the cell colonies were fixed and stained with 0.01% crystal violet for 10 min at room temperature. The colonies were subsequently visualized under an optical microscope (Olympus CKX41, Tokyo, Japan).

Wound healing assay

The wound healing assay was utilized to evaluate the effect of nuciferine on the migration of MH7A cells. Initially, MH7A cells were cultured in six-well plates until they reached 70%–80% confluence. A sterile pipette tip was then used to create a linear scratch across the cell monolayer, and the area was washed with phosphate-buffered saline to remove detached cells and debris. Subsequently, the cells were treated with nuciferine at concentrations of 0, 20, 40, and 80 μmol·L^{-1} for 24 h. Microscopic images were captured at 0 and 24 h post-injury to assess cell movement. The rate of wound closure was quantified by counting the number of cells that migrated across the scratch line.

EdU assay in vitro

EdU (5-ethynyl-2'-deoxyuridine), provided by Beyotime Biotechnology (Shanghai, China), is a novel thymidine analog that integrates into newly synthesized DNA, substituting thymidine during DNA replication. MH7A cells were pre-treated with nuciferine at concentrations of 0, 20, 40, and 80 μmol·L^{-1} for 24 h. Following the pre-treatment, EdU (10 μmol·L^{-1}) was added to each well according to the manufacturer's instructions. Subsequently, Hoechst 33342 was employed to stain the cell nuclei (blue), whereas proliferating cells incorporating EdU were stained red. The proportion of EdU-positive cells was quantified in relation to the total number of cells stained with Hoechst 33342, facilitating the assessment of cell proliferation.

EdU staining in vivo

EdU was initially dissolved in DMSO and subsequently diluted with PBS to achieve a concentration of 0.5 mg·mL^{-1}. Each group of rats was then administered an intraperitoneal dose of EdU at 5 mg·kg^{-1}. After a period of 7 h, all rats were euthanized, and their articular tissues were collected for histological analysis.

Flow cytometry

To assess the impact of nuciferine on cell cycle arrest and apoptosis in MH7A cells, flow cytometry analysis was conducted. Initially, MH7A cells were pre-treated with nuciferine at concentrations of 20, 40, and 80 μmol·L^{-1} for 24 h. Subsequently, the cells were harvested and resuspended in a binding buffer that included propidium iodide (PI) at a concentration of 10 mg·mL^{-1} and Ribonucleases (RNase) at 100 mg·mL^{-1}. This mixture was incubated at 37 °C for 20 min. A Gallios flow cytometer (Beckman Coulter, CA, USA) was then utilized to analyze the cell staining.

For apoptosis analysis, the fluorescein isothiocyanate (FITC)/Annexin V Apoptosis Detection Kit (BD Biosciences, Franklin Lakes, NJ, USA) was employed following the manufacturer's protocol. Specifically, after 24 hours of nuciferine treatment at the same concentrations, MH7A cells were stained with 5 μL of Annexin V-FITC and 5 μL of PI. The stained cells were subsequently analyzed using the Gallios flow cytometer (Beckman Coulter, CA, USA).

Transwell chamber assay

The study conducted cell migration and invasion assays using a Transwell chamber (pore size: 8 μm; Corning, Tewksbury, MA, USA), with and without a Matrigel coating, respectively. MH7A cells were treated with varying concentrations of nuciferine (20, 40, and 80 μmol·L^{-1}) for 12 h. After treatment, the cells were suspended in serum-free DMEM and seeded into the upper chamber of the Transwell apparatus. DMEM containing 20% fetal bovine serum was placed in the lower chamber to serve as a chemoattractant. For the migration assay, MH7A cells were incubated in the chambers for 24 h. In the case of the invasion assay, the chambers were pre-coated with Matrigel basement membrane matrix (BD Biosciences, Franklin Lakes, NJ, USA) to mimic the extracellular matrix barrier. Here, MH7A cells were incubated for 48 hours to allow for invasion through the Matrigel. Post-incubation, cells that migrated or invaded through the pores to the lower side of the membrane were stained with 0.1% crystal violet and visualized under an optical light microscope.

Western blotting assay

MH7A cells were pre-treated with nuciferine at concentrations of 20, 40, and 80 μmol·L^{-1} for 24 h. Subsequently, the cells were harvested and lysed in Radio-Immunoprecipitation Assay (RIPA) buffer containing protease and phosphatase inhibitors (Roche Diagnostics, Mannheim, Germany). The lysates were centrifuged at 12 000 r·min^{-1} for 15 min at 4 °C to collect the supernatants. The protein concentration in each sample was quantified using the Bicinchoninic Acid (BCA) Protein Assay Kit (Beyotime, Shanghai, China). Equal amounts of protein (30 μg) from each sample were separated by Sodium dodecyl-sulfate polyacrylamide gel electrophoresis (SDS-PAGE) and transferred onto polyvinylidene difluoride (PVDF) membranes. These membranes were blocked with 5% fat-free milk and incubated overnight at 4 °C with primary antibodies against Bcl2, Bax, Caspase3, cleaved-Caspase 3 (cleaved-CASP3), Cyclin-dependent kinase2 (CDK2), Cyclin-dependent kinase4 (CDK4), Cyclin D1 (CCND1), Cyclin E1 (CCNE1), and β-actin (1 ∶ 1000 dilution), all sourced from Cell Signal Technology (Beverly, MA, USA). Following primary antibody incubation, the membranes were washed and incubated with a horseradish peroxidase-conjugated secondary antibody (dilution 1 ∶ 5000) at room temperature for 1 h. Enhanced chemiluminescence (ECL) reagents (Amersham, Shanghai, China) were used to detect immunoreactivity according to the manufacturer's instructions. The relative protein expression levels were quantified using ImageJ software (US National Institutes of Health, Bethesda, MD, USA)

CIA rat model induction and nuciferine treatment

Female Wistar rats, aged 6–8 weeks (180–220g), were maintained under controlled conditions with a temperature of 20–22 °C, a 12-hour light/dark cycle, and 40%–60% humidity. After acclimatizing for one week, the rats were intradermally immunized at the base of the tail with 1.5 mg of native bovine collagen type II (CII; 0.2 mL) (Chondrex, Redmond, WA, USA) mixed with an equal volume of incomplete Freund's adjuvant (Chondrex) on day 0, followed by a booster immunization on day 7 [22]. The rats were categorized into five groups for the subsequent treatment phase of the CIA model, which began on day 12 post-initial immunization and continued until day 42 of the study. The treatment groups included normal rats receiving saline (Control, n = 6), CIA rats receiving 0.5% CMC-Na as a vehicle control (CIA, n = 6), low-dose nuciferine (20 mg·kg^{-1}, n = 6), high-dose nuciferine (60 mg·kg^{-1}, n = 6), and tripterygium polyglucoside as a positive control (5.4 mg·kg^{-1}, n = 6), administered daily. Hind paw volume was measured biweekly using a PV-200 toe volume meter (Chengdu DE Man, China), starting one day before immunization. Simultaneously, two independent observers who were not familiar with the treatment regimen were given the arthritis score weekly. The scoring criteria were as follows: 0) no visible signs of arthritis, swelling, or erythema; 1) local swelling or erythema; 2) local toe joints and dorsal foot involvement, leading to a maximum possible score of 16 for all four legs combined [23]. On day 42, rats were anesthetized with ether and euthanized, and tissues from spleens and hindlimbs were collected for further analysis. This study was performed in accordance with ethical guidelines approved by the Ethics Committee of Shanghai University of Traditional Chinese Medicine (Approval Number PZSHUTCM200430001, dated 30 April 2020).

Determination of cytokines and antibodies

On day 42 of the animal experiment, rats were euthanized after 2 h after receiving their last treatment. Blood samples were collected from the retro-orbital plexus, and serum was isolated by centrifugation at 3000 r·min^{-1} for 15 minutes at 4 °C. The serum samples were then stored at −80 °C until analysis. Cytokines, including TNF-α, IL-1β, and IL-6, as well as autoantibodies (IgG, IgG1, IgG2a), were quantified in the serum using enzyme-linked immunosorbent assay (ELISA) kits (MultiSciences, Hangzhou, China), following the manufacturer's provided instructions.

Histopathological examination

After micro-CT analysis, the ankle joints were excised, fixed in 10% formalin, decalcified in 12% disodium ethylenediaminetetraacetic acid (EDTA), and subsequently embedded in paraffin. Sections of paraffin-embedded tissues were stained using hematoxylin and eosin (H&E) or safranin O/fast green for microscopic examination. An investigator, who was blinded to the treatment groups, evaluated the histological sections to assign an arthritis score based on the severity of synovial proliferation, immune cell infiltration, cartilage erosion, and pannus formation. The histologic arthritis scoring system utilizes a scale ranging from 0 (no evidence) to 3 (severe), facilitating a quantitative assessment of the histo-

pathological features indicative of arthritis severity [23].

T cell isolation and Th17/Treg differentiation in the rat spleen

The spleens were homogenized using a nylon mesh to create a single-cell suspension. Red blood cells were lysed using 0.83% ammonium chloride solution, and the resulting spleen cell suspension was filtered through a 70-μm cell strainer. The cells were then treated with Brefeldin (BioLegend, CA, USA) for 6 hours to activate them. Following activation, the cells were stained with FITC-conjugated CD3, phycoerythrin (PE)-conjugated CD4, and BV421-conjugated CD25 monoclonal antibodies for surface markers. After surface staining, the cells underwent permeabilization for intracellular staining (BioLegend), which allowed for the intracellular staining with allophycocyanin (APC)-conjugated IL-17A antibody (BioLegend) to detect Th17 cells. T cells were identified by staining the lymphocytes with APC-conjugated Foxp3 antibody (BioLegend). Flow cytometry was performed to analyze the stained cells, and data analysis was carried out using FlowJo version 7.6.1 software (Tree Star, Ashland, OR, USA).

Quantitative real-time PCR (qPCR)

MH7A cells were plated in 6-well plates at a density of 1×10^5 cells/well and incubated overnight. Subsequently, the cells were treated with various concentrations of nuciferine (10, 20, 40 μmol·L^{-1}) before being stimulated with TNF-α for 24 h. Total RNA was extracted from the TNF-α-stimulated MH7A cells and a third of the spleen tissue from rats using the EZ-press RNA Purification Kit (EZBioscience, Roseville, CA, USA). cDNA synthesis was carried out at 42 °C for 15 minutes, followed by a denaturation step at 95 °C for 30 seconds using the 4 × Reverse Transcription Master Mix (EZBioscience). The qPCR reaction was conducted using the Takara SYBR Green Master Mix Kit on the ABI Prism 7900HT Sequence Detection System (Life Technologies, Carlsbad, CA, USA), following previously reported methodologies [24]. The specific genes and their primer sequences are detailed in Table 1.

Radiographic evaluation and micro-CT analysis

The hindlimbs of the rats were fixed in a 4% paraformaldehyde/phosphate-buffered saline solution, with soft tissue removed to facilitate radiological assessments and micro-CT scanning (Pingseng Healthcare Co., Kunshan, China) for the evaluation of joint damage extent. The hind paws were radiographed at 22 kV for 200 ms using the Faxitron radiography system (MultiFocus; Faxitron, Tucson, AZ, USA). Joint damage was quantified using a previously described scoring system [25]. Subsequently, the right hindlimb underwent micro-CT analysis, followed by three-dimensional reconstruction. The scanning parameters were set at 90 kV, 70 μA, and 100 ms. Trabecular parameters, including bone surface density (*Bs*/*Bv*), bone volume fraction (*Bv*/*Tv*), and trabecular thickness (*Tb.Th*; mm), were quantified utilizing the software provided by the manufacturer.

Statistical analysis

Statistical analysis was conducted using GraphPad Prism version 9.00 (GraphPad Software Inc., San Diego, CA, USA). All results are expressed as standard error of the mean (SEM), depending on the context. These data were derived from more than three separate experiments. Differences among three or more groups were evaluated using one-way analysis of variance (ANOVA). A *P*-value of less than 0.05 was considered statistically significant.

Results

Nuciferine inhibited the proliferation of MH7A cells

Abnormal hyperplasia of synovial tissue is a hallmark pathological feature in patients with RA. Thus, we explored

Table 1 Primers used for qPCR analysis

Name	Species	Forward primer (5'-3')	Reverse primer (5'-3')
Bcl-2	Homo	GCCTTCTTTGAGTTCGGT	GCCGTACAGTTCCACAAA
Bax	Homo	GTCGCCCTTTTCTACTTTG	GGACATCAGTCGCTTCAGT
Ccnd1	Homo	TCCTACTACCGCCTCACA	ACCTCCTCCTCCTCCTCT
Ccne1	Homo	GCCTTGTATCATTTCTCGTC	GCTGTCTCTGTGGGTCTG
β-Actin	Homo	GACATCCGCAAAGACCTG	GGAAGGTGGACAGCGAG
CDK4	Homo	AAGTTGACGGGAGAGGTG	AATGCCAGTGAGAGCAGA
CDK2	Homo	CCAGGAGTTACTTCTATGCCTGA	TTCATCCAGGGGAGGTACAAC
GAPDH	Rat	TGGAGAAACCTGCCAAGTATGA	CTCTCAGCTGTGGTGGTGAA
RORγt	Rat	CTGCAATACAATTTGGAGCTG	GTGGAGGTGCTGGAAGTC
IL-17A	Rat	TCACAGTTGAATCTCAGCAAG	GCCCACAGAAAAACAAGAAG
Foxp3	Rat	AGGCACATCAGGCACTAAGGTT	AATGGGAAGGGGAATGGAGA
IL-10	Rat	TGCATAGAAGCCTACGTGACA	TGGAGAGAGGTACAAACGAGG
GAPDH	Homo	GAGTCAACGGATTTGGTCGT	GACAAGCTTCCCGTTCTCAG
IL-1β	Homo	GATATGGAGCAACAAGTGGT	AGGACAGGTACAGATTCTTTTC
IL-6	Homo	TAGGACTGGAGATGTCTGAGG	TGTGGAGAAGGAGTTCATAGC
MMP2	Homo	TACAACTTCTTCCCTCGCAAG	AAAGGCATCATCCACTGTCTC
MMP9	Homo	GCTGGGCTTAGATCATTCCTC	ATTCACGTCGTCCTTATGCAA

the effects of nuciferine on the cell viability of the RA patient-derived fibroblast-like synoviocyte (FLS) cell line, MH7A. MH7A cells possess several characteristics typical of FLS cells in RA, such as the capacity for proliferation, invasion, and the secretion of cytokines and matrix metalloproteinases, making them a suitable *in vitro* model for investigating RA pathogenesis and evaluating potential therapeutic agents. Our findings demonstrated that nuciferine significantly reduced the viability of MH7A cells in a concentration-dependent manner (Fig. 1B), indicating its potential antiproliferative effects on FLS cells. To further explore the suppressive impact of nuciferine on MH7A cells, a colony formation assay was performed, which also serves as an indicator of cell proliferation capability. The results indicated that nuciferine reduced the number of colonies in a dose-dependent manner (Fig. 1C). Additionally, the effects of nuciferine on single-cell proliferation were assessed using a 5-Ethynyl-2'-deoxyuridine (EdU) assay, which corroborated that nuciferine dose-dependently inhibited the proliferation of MH7A cells (Fig. 1D).

Nuciferine promoted apoptosis and induced G_1/S phase arrest of MH7A cells

Given that promoting apoptosis and inducing cell cycle arrest in fibroblast-like synoviocytes (FLS) cells are beneficial strategies for treating arthritis, we investigated the effects of nuciferine on the cell cycle of MH7A cells using flow cytometry. The results showed that nuciferine induced G_1/S phase arrest, significantly increasing the proportion of cells in the G_1 phase and decreasing those in the S and G_2 phases

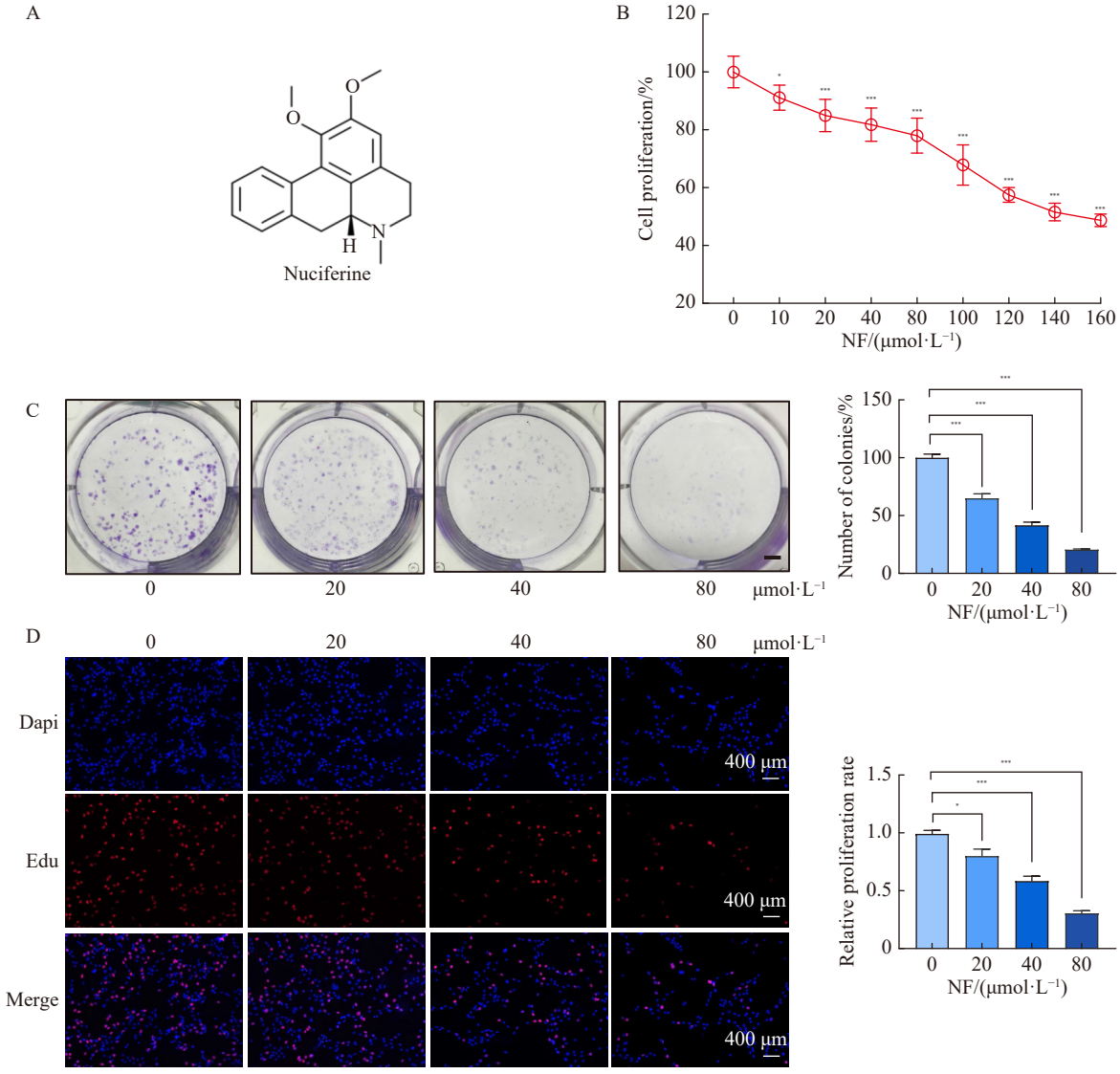

Fig. 1 Nuciferine inhibits the proliferative activity of MH7A cells. (A) Chemical structural formula of nuciferine. (B) Results of Cell Counting Kit-8 (CCK-8) assay showing reduced viability of MH7A cells after 24 h of exposure to nuciferine. (C) Inhibitory effect of nuciferine on the colony formation of MH7A cells. (D) Representative images of EdU assay demonstrating inhibition of single-cell proliferation of MH7A cells by nuciferine. Proliferating cells are labeled in red (EdU), and cell nuclei are stained in blue (DAPI). All values are presented as mean ± standard error of the mean (SEM) from at least three independent experiments ($n = 3$). $^{*}P < 0.05$, $^{**}P < 0.001$ *vs* control cells.

(Fig. 2A). We also examined the expression levels of critical cell mitosis regulators, including cyclins and cyclin-dependent kinases (CDKs), and discovered that nuciferine dose-dependently diminished the protein and mRNA levels of Cyclin D1 *(CCND1*), Cyclin E1 (*CCNE1*), CDK2, and CDK4 (Fig. 2B). Additionally, apoptosis analysis in cells treated

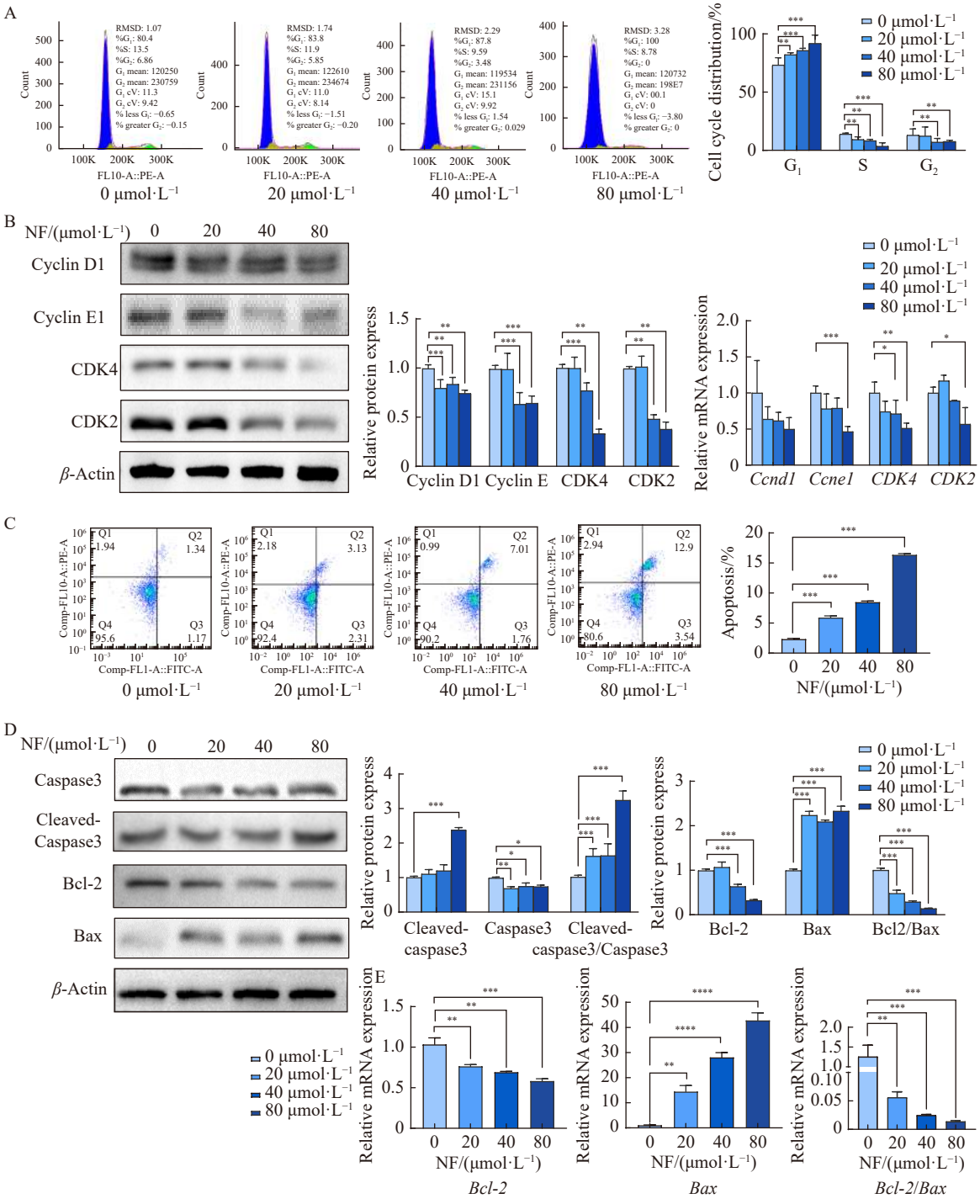

Fig. 2 Nuciferine induces apoptosis and cell cycle arrest in MH7A cells. (A) Flow cytometry analysis showing the effect of nuciferine on cell cycle arrest in MH7A cells. (B) Western blotting and quantitative real-time PCR (qPCR) were used to determine the expression levels of cell cycle-related proteins. (C) Flow cytometry analysis showing the pro-apoptotic effect of nuciferine on MH7A cells. (D) Western blotting was used to determine the expression levels of apoptosis-related proteins. (E) qPCR was used to examine the mRNA expression levels of *Caspase-3*, *Bcl-2*, and *Bax* in nuciferine-treated MH7A cells. All values are presented as mean ± standard error of the mean (SEM) from at least three independent experiments ($n = 3$). $P < 0.05$, $P < 0.01$, $P < 0.001$ *vs* control cells.

with nuciferine revealed a concentration-dependent augmentation in the percentage of apoptotic cells (Fig. 2C). was noted with nuciferine treatment, leading to an elevated ratio of cleaved-CASP3 to CASP3 (Fig. 2D). Further evaluation of apoptosis-related proteins indicated that nuciferine downregulated the expression of the anti-apoptotic protein Bcl-2 and upregulated the expression of the pro-apoptotic protein Bax (Figs. 2D and 2E).

Nuciferine inhibited the invasion and migration of MH7A cells

Prior research has indicated that inhibiting the migratory and invasive capabilities of FLS could be a viable approach to mitigate the progressive damage to cartilage and bone seen in arthritis [26]. To assess the effects of nuciferine on FLS cell migration, a transwell migration assay was performed. The findings revealed a decrease in the migration percentage of MH7A cells correlating with increasing concentrations of nuciferine (Fig. 3A). Additionally, to further validate the impact of nuciferine on MH7A cell migration, a monolayer wound scratch assay was executed. The results demonstrated that nuciferine dose-dependently reduced the migration of MH7A cells (Fig. 3B). Moreover, the ability of nuciferine to curb the invasiveness of MH7A cells was confirmed through a transwell invasion assay, showcasing its inhibitory effect (Fig. 3C).

Nuciferine decreased the pro-inflammatory mediators in MH7A cells

Subsequently, an RT-qPCR assay was utilized to explore the effects of nuciferine on the expression of inflammatory mediators in TNF-α-stimulated MH7A cells. The results indicated that TNF-α stimulation elevated the mRNA levels of *IL-1β*, *IL-6*, *Mmp-2*, and *Mmp-9* in MH7A cells. Nonetheless, treatment with nuciferine markedly decreased the expression of these pro-inflammatory mediators in a dose-dependent fashion (Figs. 4A–4D).

Nuciferine ameliorated joint destruction in CIA rats

The therapeutic potential of nuciferine for arthritis was evaluated in a CIA rat model (Fig. 5A). Seven days following the initial immunization, all groups, except the control, exhibited pronounced pathological symptoms including joint redness and swelling, movement disorders, and dull skin color (Fig. 5B). However, rats administered with nuciferine (20 and 60 mg·kg^{-1}) and a positive control drug (5.4 mg·kg^{-1}) displayed significantly mitigated arthritis symptoms. The extent of paw joint swelling in the treatment groups progressively increased, peaking between 14 to 21 days post-immunization, in contrast to the control group (Fig. 5C). Notably, rats receiving low (20 mg·kg^{-1}) and high (60 mg·kg^{-1}) doses

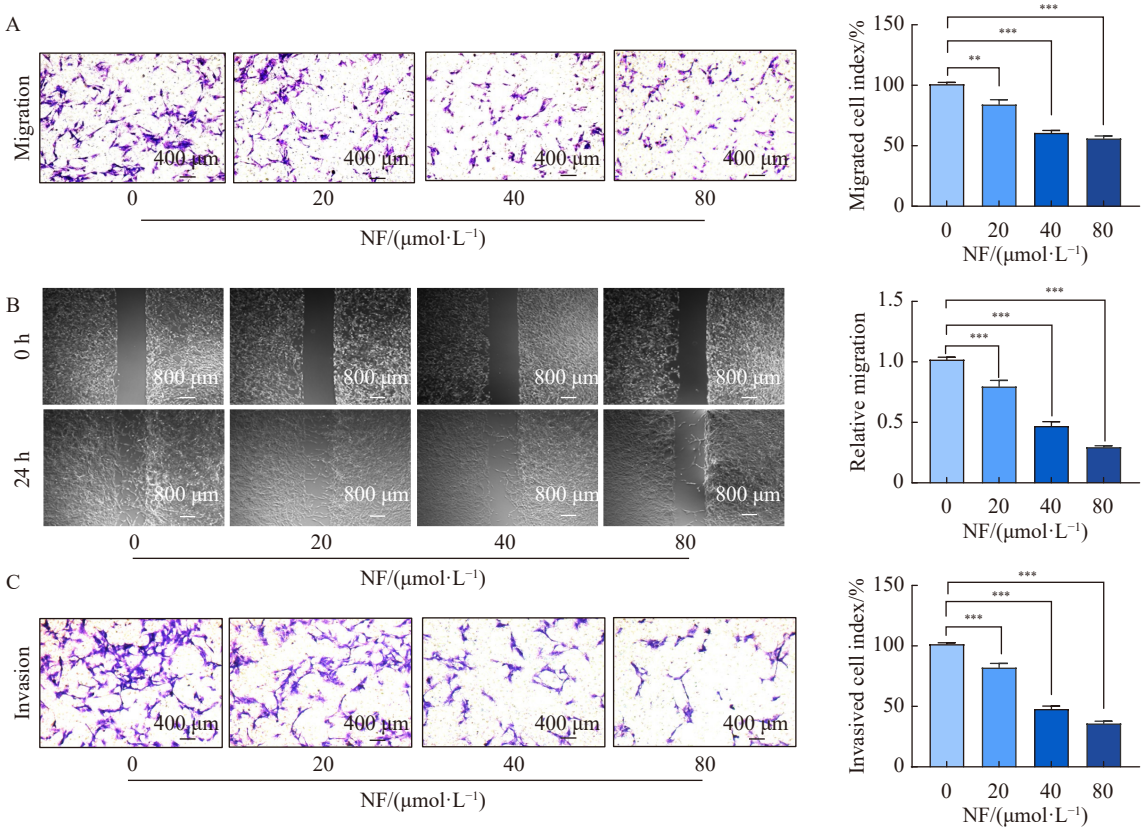

Fig. 3 Nuciferine inhibits the migration and invasion of MH7A cells. (A) A modified Boyden chamber test was conducted to measure the cell migration viability of MH7A cells after exposure to nuciferine. (B) Wound-healing assay was performed to further detect the cell migration viability of MH7A cells after nuciferine treatment. (C) Matrigel-coated transwell assay was used to examine the cell invasion ability of MH7A cells. All data are presented as mean ± SEM (n = 3) from three independent experiments. Statistical significance is indicated as follows: $^{**}P < 0.01$, $^{***}P < 0.001$ *vs* control cells.

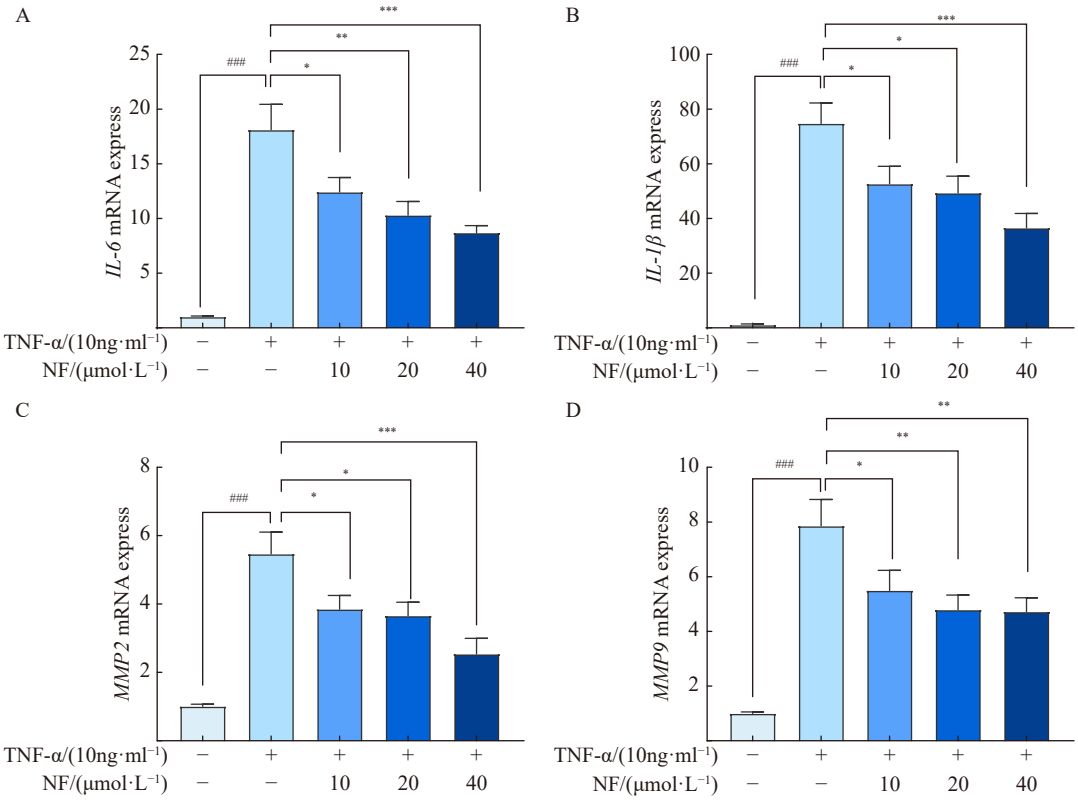

Fig. 4 Nuciferine suppresses the mRNA expression of pro-inflammatory cytokines in TNF-α-treated MH7A cells. (A–D) The mRNA expression levels of *IL-6*, *IL-1β*, *Mmp-2*, and *Mmp-9* were measured using qPCR in nuciferine-treated MH7A cells. *β*-Actin was used as the internal control. Data are presented as the mean ± SEM (n = 3). $^{\#\#\#}P < 0.001$ *vs* vehicle-treated cells; $^{*}P < 0.05$, $^{**}P < 0.01$, $^{***}P < 0.001$ *vs* TNF-α-treated cells.

of nuciferine, as well as the positive control, exhibited significantly reduced paw volume and arthritis scores (Figs. 5C and D). Histopathological changes in the hind right paw joints were assessed through safranin O/fast green and HE staining (Fig. 6A), revealing that both low and high doses of nuciferine, alongside the positive control, considerably improved histopathological conditions. Synovial hyperplasia, cartilage damage, inflammatory cell infiltration, and synovial tissue erosion were substantially less severe in the groups treated with nuciferine and the positive control compared to the CIA rats (Fig. 6B). Additionally, Edu staining assays indicated pronounced synovial cell proliferation in CIA rats, whereas nuciferine treatment at both low and high doses notably inhibited synovial cell proliferation (Fig. 6A). Corroborating these observations, the release of pro-inflammatory cytokines (TNF-α, IL-1β, and IL6) and levels of IgG, including isotype-specific IgG1 and IgG2a in CIA rats, were significantly reduced in the nuciferine-treated groups and the positive control group (Figs. 6C and 6D).

Radiographic assessments were performed to elucidate the effects of nuciferine on joint damage in CIA rats. Under X-ray images of the hind paws from CIA, rats displayed characteristic signs of severe joint damage, including pronounced joint deformity, articular destruction, and narrowing of the joint space (Fig. 7A). Radiological examination and scoring demonstrated a significant reduction in joint destruction among rats treated with nuciferine and the positive control drug. Further, micro-CT scanning and three-dimensional reconstruction analyses were employed to closely examine the impact of nuciferine on bone deterioration (Fig. 7B). Key trabecular bone parameters, such as *Bv* relative to *Tv*, and trabecular thickness (*Tb.Th*) were significantly diminished, while the measure of surface density (bone surface [*Bs*]/bone volume [*Bv*]) was substantially reduced in the CIA model group (Fig. 7C). Treatment with nuciferine and the positive control effectively ameliorated these parameters, indicating an improvement in bone integrity and a mitigation of bone destruction.

Nuciferine rectified the imbalance of Th17/Treg cells in CIA rats

To explore the potential regulatory impact of nuciferine on the Th17/Treg cell imbalance in CIA rats, we assessed the frequencies of Th17 and T cells within the spleen. The analysis revealed a significantly elevated proportion of $CD4^{+}IL\text{-}17A^{+}$ T cells in CIA rats compared to controls, indicating an increase in Th17 cell populations in the spleens of CIA rats (Fig. 8A). In contrast, the proportion of $CD25^{+}Foxp3^{+}$ T cells was notably lower in CIA rats than in control animals, suggesting a decrease in T cell numbers in the spleens of CIA rats (Fig. 8B). Treatment with nuciferine and the positive control drug significantly corrected the Th17/Treg cell imbalance observed in CIA rats.

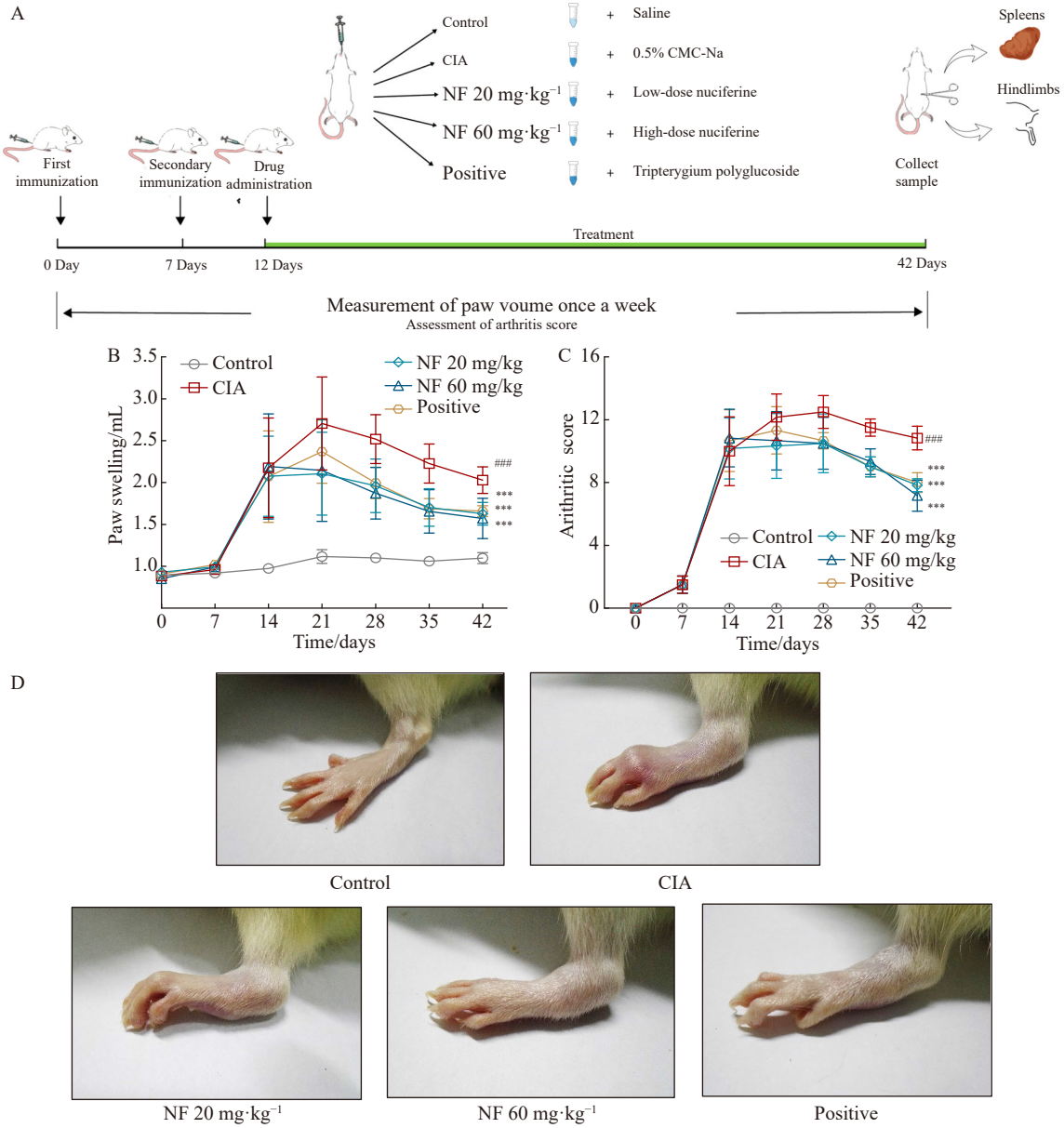

Fig. 5 Nuciferine alleviates disease progression in collagen-induced arthritic (CIA) rats. (A) Experimental design for the rat study. (B) Nuciferine treatment reduced paw joint swelling in CIA rats. (C) Nuciferine treatment improved arthritis scores in the hind paws of CIA rats. (D) Representative images of hind paws. Data are presented as the mean ± SEM (n = 6). $^{###}P < 0.001$ *vs* Control; $^{***}P < 0.001$ *vs* the CIA model group.

To delve deeper into whether nuciferine corrects the Th17/Treg ratio imbalance in the spleens of CIA rats by influencing the differentiation-related transcription factors of Th17 and T cells, we evaluated the mRNA expression levels of cytokines (*Il-17* and *Il-10*) and differentiation-related transcription factors (retinoic acid receptor-related orphan receptor gamma t [*RORγt*] for Th17 cells and forkhead box P3 [*Foxp3*] for T cells) in the spleen. The findings demonstrated that nuciferine treatment led to a significant reduction in the mRNA levels of *Il-17* and *RORγt*, indicative of a decrease in Th17 cell differentiation. Conversely, the mRNA levels of *Foxp3* and *Il-10*, which are associated with T cell differentiation, were significantly increased following nuciferine administration (Fig. 8C).

Discussion

RA is a complex autoimmune disorder marked by chronic inflammation, leading to joint destruction. The pathology of RA is underpinned by dysregulated signaling pathways and the involvement of various immune cells that perpetuate inflammation and joint damage [27]. While corticosteroids and DMARDs have been the cornerstone of RA treatment, their effectiveness is often limited [28, 29]. Nuciferine, a bioactive alkaloid, is recognized for its diverse pharmacological properties, including antioxidative, antibacterial, anti-inflammatory, and anti-tumor effects [17-20]. In our research, we identified a

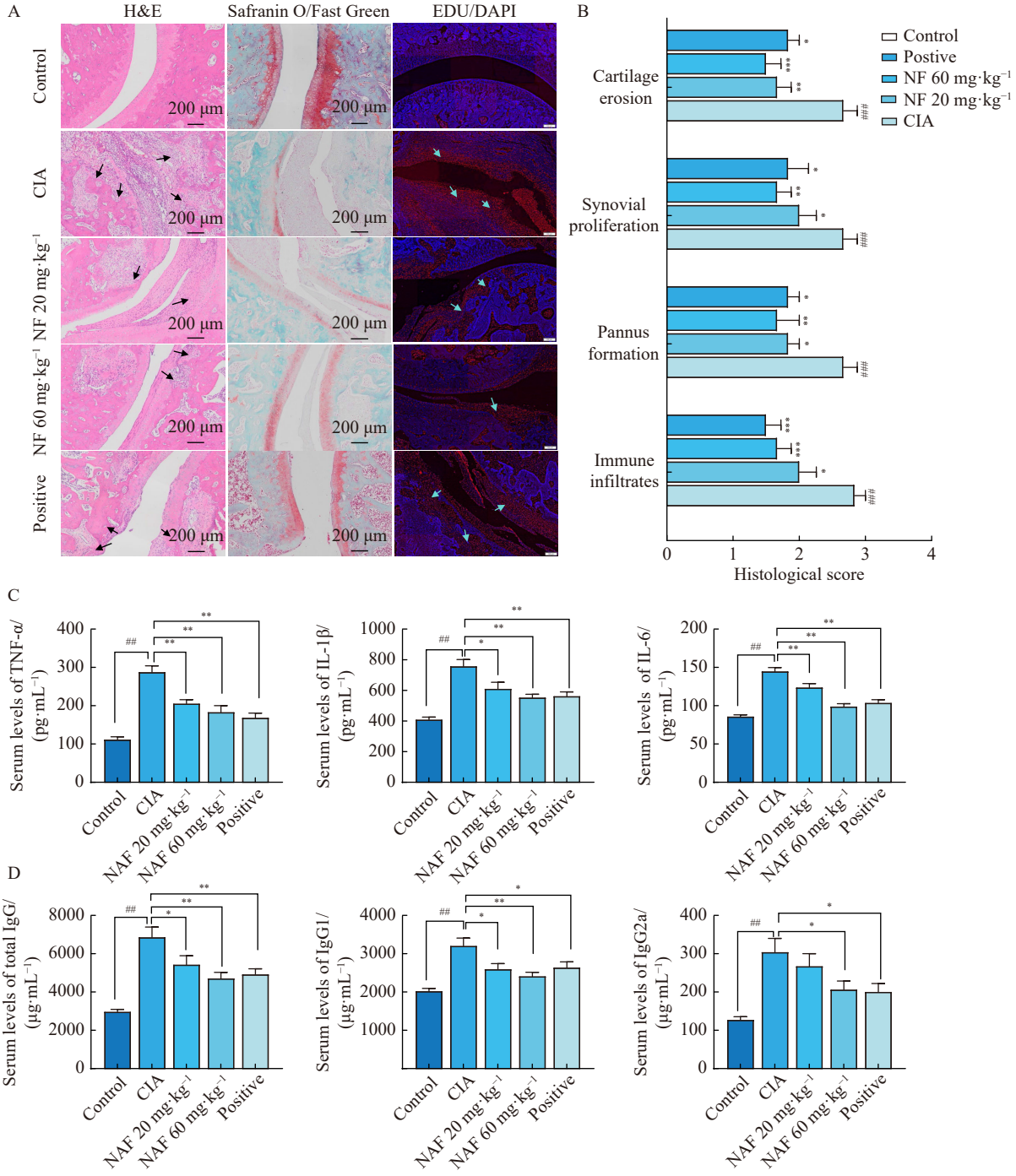

Fig. 6 Nuciferine reduces pathological injury and inflammatory cytokine release in CIA rats. (A) Representative H&E and safranin O/fast green sections and Edu staining (40 ×) of rat ankles from different groups. (B) Histopathological score of rats in each group. (C) Serum levels of TNF-α, IL-1β, and IL-6 in each group of rats were measured by ELISA. (D) Serum total IgG, isotype-specific IgG1, and IgG2a in each group of rats were determined by ELISA. Data are presented as the mean ± SEM (n = 6). $^{\#\#}P < 0.01$, $^{\#\#\#}P < 0.001$ *vs* Control; $^{*}P < 0.05$, $^{**}P < 0.01$, $^{***}P < 0.001$ *vs* the CIA model group.

novel pharmacological action of nuciferine in inhibiting the proliferation and invasiveness of FLS and reducing joint damage in CIA rats.

The hyperplasia of FLS is fundamentally implicated in the pathogenesis of RA [5, 8], where FLS cells from RA patients manifest tumor-like characteristics, including enhanced proliferation, migration, and invasiveness [30]. Notably, nuciferine has previously demonstrated antiproliferative effects on non-small cell lung cancer and glioblastoma cells [18, 31]. In our investigation, nuciferine was found to significantly inhibit the proliferation of FLS cells derived from RA patients, as evidenced by reductions in cell viability,

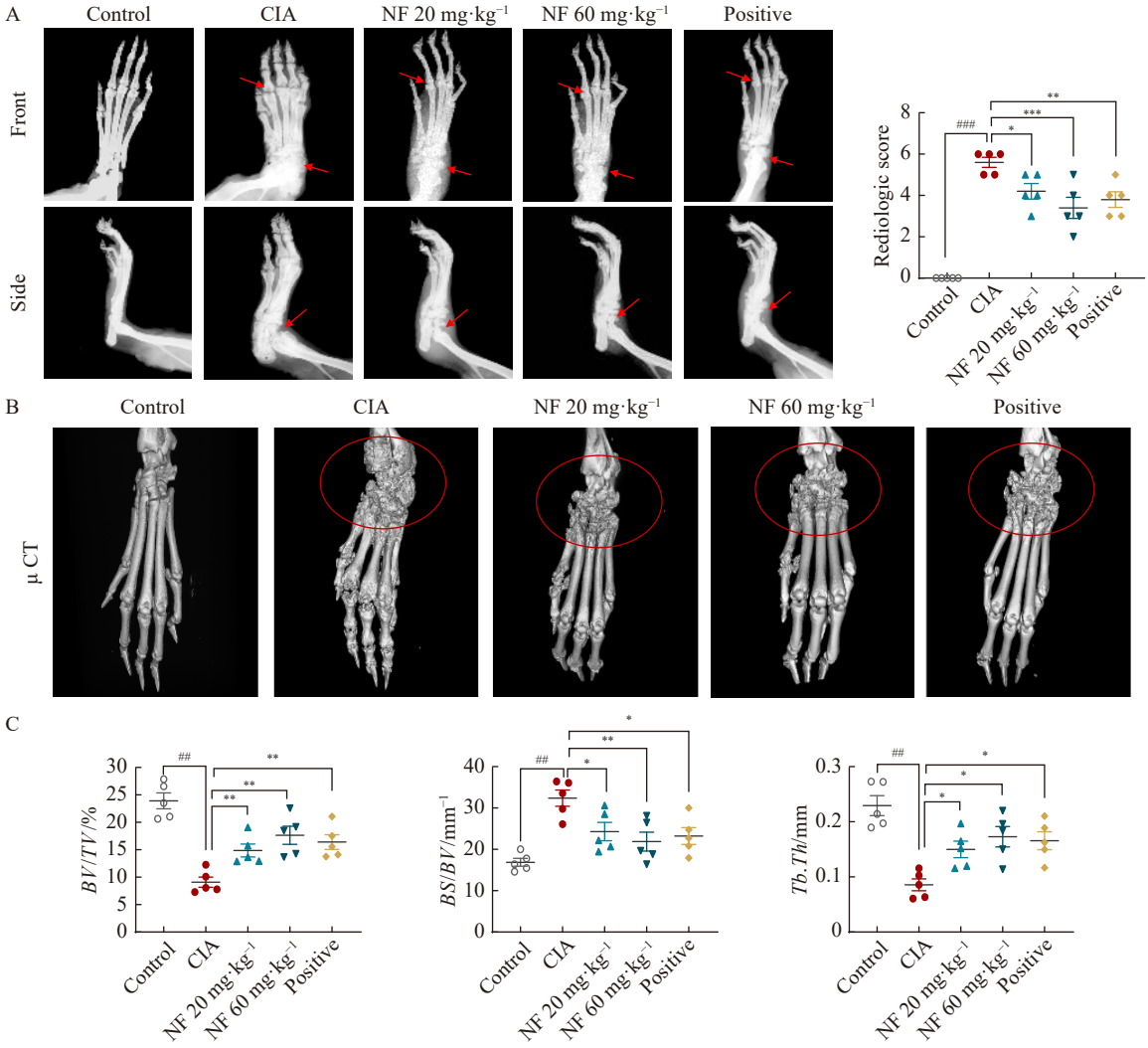

Fig. 7 Nuciferine reduces joint destruction in CIA rats. (A) Representative radiographs of hind paws and radiological scores. (B) Representative reconstructed 3D micro-CT images of right hind paw joints showing the degree of joint bone erosion. (C) Micro-CT analysis of surface density (*Bs*/*Bv*), trabecular bone volume (*Bv*/*Tv*), and trabecular thickness (*Tb.Th*). Data are presented as the mean ± SEM ($n = 5$). $^{\#\#\#}P < 0.001$ *vs* Control; $^{*}P < 0.05$, $^{**}P < 0.01$, $^{***}P < 0.001$ *vs* the CIA model group.

colony formation, and EdU incorporation. FLS cells in RA are known for their anchor-independent growth, primarily driven by cell cycle dysregulation and an augmented resistance to apoptosis, making the regulation of the FLS cell cycle a targeted approach for RA treatment [32]. Therefore, regulation of the FLS cell cycle has become a strategy for RA treatment [6, 33]. Cell cycle progression, particularly from the early to mid G_1 phase and from the late G_1 to S phase [34, 35], is facilitated by the regulatory proteins CDK4, Cyclin D1, CDK2, and Cyclin E1. Our findings revealed that nuciferine effectively induced G_1/S arrest in FLS cells by downregulating the expression of key cell cycle regulatory genes (*CCND1*, *CCNE1*, *CDK2*, and *CDK4*).

Apoptosis, a crucial self-defense mechanism, is regulated by specific genes, with impaired programmed cell death in response to apoptotic signals marking the abnormal activation of FLS cells in RA [6, 36]. This study discovered that nuciferine effectively promotes the apoptosis of FLS cells. The proto-oncogene Bcl-2, prominently expressed in mitochondria, plays a key role in inhibiting cell apoptosis. In contrast, the tumor suppressor gene Bax facilitates apoptosis. Therefore, the Bax/Bcl-2 ratio is critical in determining cell susceptibility to drug-induced apoptosis [37, 38]. Furthermore, the activation of Caspase-3 through cleavage, a significant event in apoptotic cell death, is indicated by the ratio of cleaved-caspase-3 to total Cleaved-CASP3/CASP3, serving as a measure of apoptosis [39]. In our findings, nuciferine treatment led to an increase in both the Bax/Bcl-2 and cleaved-CASP3/CASP3 ratios in FLS cells, underscoring nuciferine's pro-apoptotic influence on FLS cells.

Aberrant intracellular signaling in osteoclasts and fibroblast-like synoviocytes (FLS) is pivotal to the bone destruction observed in RA, making the correction of these dysfunctional signals an attractive therapeutic target [40]. Beyond their proliferative behavior, the relentless invasion and adhesion of FLS cells to cartilage play a significant role in the progress-

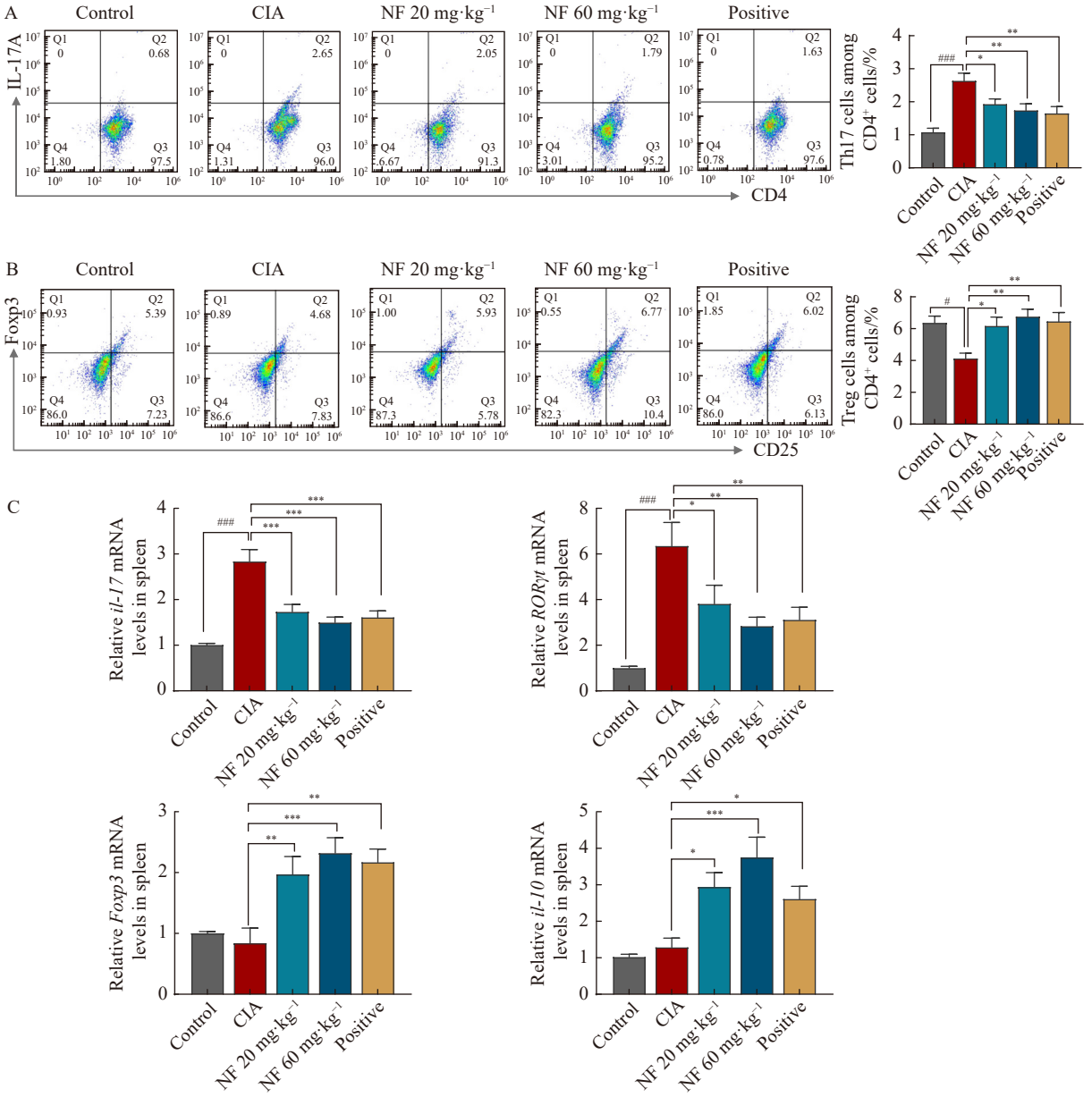

Fig. 8 Nuciferine rebalances Th17/Treg cell proportions in the spleen of CIA rats. Flow cytometric analysis of T cell subsets gated on CD4$^+$ T cells from the spleen to label Th17 cells (A) and Treg cells (B). (C) qPCR was used to measure mRNA expression of *Il-17A*, *Il-10*, *RORγt*, and *Foxp3* in the spleen. Data are presented as the mean ± SEM (n = 6). $^{\#}P < 0.05$, $^{\#\#\#}P < 0.001$ vs Control; $^{*}P < 0.05$, $^{**}P < 0.01$, $^{***}P < 0.001$ *vs* the CIA model group.

ive degradation of cartilage and bone [41]. Thus, inhibiting the invasive capacity of FLS cells in synovial tissues could markedly mitigate the pathogenic progression of RA [41, 42]. In our research, nuciferine demonstrated potent inhibitory effects on the migration and invasion of FLS cells. Prior studies have linked the invasiveness of FLS cells to the overexpression of MMPs within the inflammatory milieu [42, 43]. Activated FLS cells engage robustly with the extracellular matrix, adhering to and invasively degrading cartilage and bone [44, 45]. Our findings indicate that nuciferine reduced the mRNA levels of adhesion molecules *Mmp-2* and *Mmp-9* in TNF-α-induced FLS cells. Furthermore, activated FLS cells release various pro-inflammatory mediators that attract macrophages, T cells, and B cells to the joints, thereby exacerbating synovial inflammation, cartilage erosion, and joint damage. Previous reports have highlighted nuciferine's capacity to suppress pro-inflammatory factor expression induced by lipopolysaccharide (LPS) in mouse mammary epithelial cells [46]. Consistent with expectations, nuciferine treatment significantly lowered the mRNA levels of *Il-1β* and *Il-6* in TNF-α-stimulated FLS cells, suggesting its potential to attenuate synovial inflammation and consequent joint damage in RA.

We proceeded to assess the potential effects of nuciferine on a rat model of RA. Among various chemical-induced models of RA, both CIA and adjuvant-induced arthritis models are widely recognized [47]. However, the CIA model is

deemed more closely aligned with human RA pathology, characterized by synovial hyperplasia, inflammatory responses, joint damage, and deformity [48]. Consequently, we utilized the CIA rat model to explore nuciferine's effects on experimental RA. Nuciferine markedly reduced paw swelling, synovial proliferation, cartilage damage, immune cell infiltration, and erosion of synovial tissues in CIA rats. It also diminished serum levels of pro-inflammatory cytokines (TNF-α, IL-1 β, and IL-6) and IG (total IgG, isotype-specific IgG1, and IgG2a) in CIA rats. Significant bone erosion in RA is typically indicated by reduced bone mass, which can be quantitatively assessed through bone indices such as *Bv*/*Tv*, *Bs*/*Bv*, and *Tb.Th* decreases [45]. Nuciferine effectively reversed these indicators in CIA rats, demonstrating its potential to protect against cartilage and bone erosion, thereby highlighting its therapeutic benefits in RA management.

Furthermore, RA is typified by synovial hyperplasia and pannus formation, phenomena that are driven by the proliferation of FLS cells and the infiltration of immune cells [49]. This process promotes the recruitment of leukocytes, activation of immune cells, and the production of inflammatory mediators, intensifying joint damage [50]. The progression of RA, an autoimmune disease, is intertwined with the activation of these immune cells [51]. $CD4^+$ T lymphocytes can differentiate into various effector Th cells, including Th1, Th2, Th17, and regulatory T cells, influenced by the surrounding cytokine milieu [52]. The equilibrium between Th17 and T cells is crucial for managing inflammation and maintaining tolerance in autoimmune conditions. Th17 cells exacerbate RA's inflammatory response by secreting pro-inflammatory cytokines, whereas T cells contribute to self-tolerance and protection against autoimmunity [53]. In our studies, nuciferine effectively modulated the imbalance between the overactive Th17 cells and the underrepresented T cells in the spleen of CIA rates. This balance is significantly influenced by the local cytokine environment [54]. For instance, the cytokine IL-17, which is pivotal in Th17 cell proliferation and differentiation, also promotes the secretion of MMPs into synovial tissue, causing cartilage damage [55]. On the other hand, the immunosuppressive cytokine IL-10, crucial for T cell differentiation, plays a key role in alleviating arthritis symptoms [55]. In harmony with this mechanism, nuciferine was observed to decrease IL-17 levels while elevating IL-10 levels in CIA rats. Moreover, the lineage-specific transcription factors RORγt and Foxp3, which are instrumental in Th17 and T cell differentiation, respectively, were also modulated by nuciferine. Specifically, nuciferine suppressed RORγt and IL-17 expression and enhanced Foxp3 and IL-10 expression, aiding in the reestablishment of the Th17/Treg cell balance in CIA rats.

Conclusion

In summary, our findings indicate that nuciferine holds therapeutic promise for RA. The beneficial effects observed in CIA rats can primarily be linked to nuciferine's ability to correct the imbalance between Th17 and Treg cells. Furthermore, nuciferine has demonstrated efficacy in inhibiting the proliferation and invasion of synovial fibroblasts, which likely contributes to its mitigating effects on arthritis. A schematic representation of nuciferine's mechanism of action in CIA rats is provided in Fig. 9. These insights high-

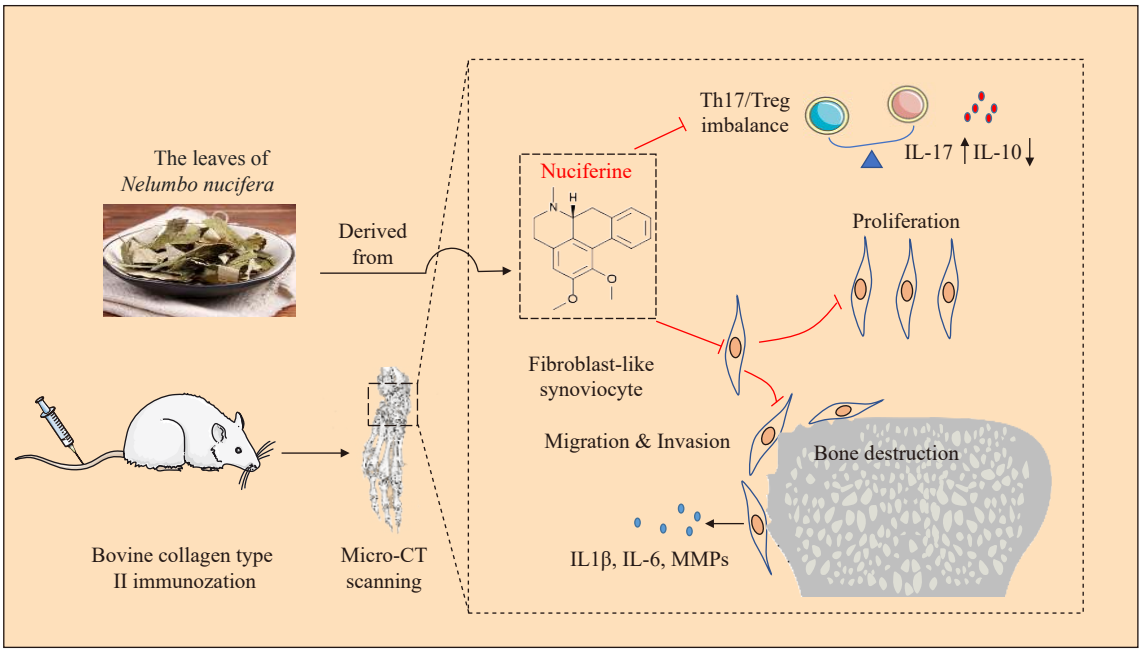

Fig. 9 Proposed mechanism for the alleviation of joint damage in collagen-induced arthritic rats by nuciferine. Firstly, nuciferine corrects the imbalance between Th17 and Treg cells by upregulating IL-17 expression and downregulating IL-10 expression. Secondly, nuciferine inhibits the proliferation of FLS cells by inducing apoptosis in MH7A cells and cell cycle arrest in MH7A cells. Consistent with these effects, nuciferine inhibits FLS cell migration and invasion, reduces FLS-induced bone destruction, and decreases the production of IL-1, IL-6, and MMP.

light the potential of nuciferine as a valuable therapeutic option for RA.

References

[1] Scott DL, Wolfe F, Huizinga TW. Rheumatoid arthritis [J]. *Lancet*, 2010, **376**: 1094-1108.

[2] Smolen JS, Aletaha DI, McInnes B, Rheumatoid arthritis [J]. ***Lancet***, 2016. **388**, 2023–2038.

[3] Scherer HU, Häupl T, Burmester GR. The etiology of rheumatoid arthritis [J]. *Autoimmun*, 2020, **110**: 102400.

[4] Tu J, Hong W, Zhang P, *et al*. Ontology and function of fibroblast-like and macrophage-like synoviocytes: how do they talk to each other and can they be targeted for rheumatoid arthritis therapy [J]. ***Front Immunol,*** **9**, 1467.

[5] You S, Koh JH, Leng L, *et al*. The tumor-like phenotype of rheumatoid synovium: molecular profiling and prospects for precision medicine [J]. *Arthritis Rheumatol*, 2018, **70**: 637-652.

[6] Malemud CJ, Matrix metalloproteinases and synovial joint pathology [J]. ***Prog Mol Biol Transl Sci***, 2017, **148**, 305–325.

[7] Xue M, McKelvey K, Shen K, *et al*. Endogenous MMP-9 and not MMP-2 promotes rheumatoid synovial fibroblast survival, inflammation and cartilage degradation [J]. *Rheumatology (Oxford)*, 2014, **53**: 2270-2279.

[8] McInnes IB, Schett G. Schett, The pathogenesis of rheumatoid arthritis [J]. *N Engl J Med*, 2011, **365**: 2205-2219.

[9] Shen P, Jiao Y, Miao L, *et al*. Immunomodulatory effects of berberine on the inflamed joint reveal new therapeutic targets for rheumatoid arthritis management [J]. *J Cell Mol Med*, 2020, **24**: 12234-12245.

[10] Weyand CM, Goronzy JJ. Goronzy, Immunometabolism in the development of rheumatoid arthritis [J]. *Immunol Rev*, 2020, **294**: 177-187.

[11] Shi C, Zhang H, Wang X, *et al*. Cinnamtannin D1 attenuates autoimmune arthritis by regulating the balance of Th17 and treg cells through inhibition of aryl hydrocarbon receptor expression [J]. *Pharmacol Res*, 2020, **151**: 104513.

[12] Jin S, Chen H, Li Y, *et al*. Maresin 1 improves the Treg/Th17 imbalance in rheumatoid arthritis through miR-21 [J]. *Ann. Rheum Dis*, 2018, **77**: 1644-1652.

[13] Batko B, Batko K, Krzanowski M, *et al*. Physician adherence to treat-to-target and practice guidelines in rheumatoid arthritis [J]. *J Clin Med*, 2019, **8**: 1416.

[14] Baschant U, Lane NE, Tuckermann J, *et al*. The multiple facets of glucocorticoid action in rheumatoid arthritis [J]. *Nat Rev Rheumatol*, 2012, **8**: 645-655.

[15] Sharma BR, Gautam LNS, Adhikari D, *et al*. A Comprehensive Review on Chemical Profiling of Nelumbo Nucifera: Potential for Drug Development [J]. *Phytother Res*, 2017, **31**(1): 3-26.

[16] Zhang C, Deng J, Liu D, *et al*. Nuciferine ameliorates hepatic steatosis in high-fat diet/streptozocin-induced diabetic mice through a PPARα/PPARγ coactivator-1α pathway [J]. *Br J Pharmacol*, 2018, **175**(21): 4218-4228.

[17] Li Z, Chen Y, An T, *et al*. Nuciferine inhibits the progression of glioblastoma by suppressing the SOX2-AKT/STAT3-Slug signaling pathway [J]. *J Exp Clin Cancer Res*, 2019, **38**(1): 139.

[18] Nguyen KH, Ta TN, Pham TH, *et al*. Nuciferine stimulates insulin secretion from beta cells-an in vitro comparison with glibenclamide [J]. *J Ethnopharmacol*, 2012, **142**(2): 488-495.

[19] Wang MX, Zhao XJ, Chen TY, *et al*. Nuciferine alleviates renal injury by inhibiting inflammatory responses in fructose-fed rats [J]. *J Agric Food Chem*, 2016, **64**(40): 7899-7910.

[20] Song C, Cao J, Lei Y, *et al*. Nuciferine prevents bone loss by disrupting multinucleated osteoclast formation and promoting type H vessel formation [J]. *FASEB J*, 2020, **34**(4): 4798-4811.

[21] Wang T, Li J, Jin Z, *et al*. Dynamic Frequency of Blood CD4 + CD25 + Regulatory T Cells in Rats with Collagen-induced Arthritis [J]. *Korean J Physiol Pharmacol*, 2015, **19**(1): 83-8.

[22] Chang Y, Wu Y, Wang D, *et al*. Therapeutic effects of TACI-Ig on rats with adjuvant-induced arthritis via attenuating inflammatory responses [J]. *Rheumatology (Oxford)*, 2011, **50**(5): 862-870.

[23] Chen R, Xie P, Gu M, *et al*. Long noncoding RNA LBC inhibits self-renewal and chemoresistance of bladder cancer stem cells through epigenetic silencing of SOX2 [J]. *Clin Cancer Res*, 2019, **25**(5): 1389-1403.

[24] Du F, Lü LJ, Fu Q, *et al*. T-614, a novel immunomodulator, attenuates joint inflammation and articular damage in collagen-induced arthritis [J]. *Arthritis Res Ther*, 2008, **10**(6): R136.

[25] Nygaard G, Firestein GS. Restoring synovial homeostasis in rheumatoid arthritis by targeting fibroblast-like synoviocytes [J]. *Nat Rev Rheumatol*, 2020, **16**(6): 333-348.

[26] Bottini N, Firestein GS. Duality of fibroblast-like synoviocytes in RA: passive responders and imprinted aggressors [J]. *Nat Rev Rheumatol*, 2013, **9**(1): 24-33.

[27] Yates M, MacGregor AJ, Ledingham J, *et al*. Variation and implications of treatment decisions in early rheumatoid arthritis: results from a nationwide cohort study [J]. *Rheumatology (Oxford)*, 2020, **59**(8): 2035-2042.

[28] Chinese Rheumatology Association. [2018 Chinese guidelines for the diagnosis and treatment of rheumatoid arthritis]. ***Zhonghua Nei Ke Za Zhi***, 2018, 57(4): 242-251. Chinese.

[29] Liu W, Yi DD, Guo JL, *et al*. Nuciferine, extracted from Nelumbo nucifera Gaertn, inhibits tumor-promoting effect of nicotine involving Wnt/β-catenin signaling in non-small cell lung cancer [J]. *J Ethnopharmacol*, 2015, **165**: 83-93.

[30] Pap T, Müller-Ladner U, Gay RE, *et al*. Fibroblast biology. Role of synovial fibroblasts in the pathogenesis of rheumatoid arthritis [J]. *Arthritis Res*, 2000, **2**(5): 361-367.

[31] Satyanarayana A, Kaldis P. Mammalian cell-cycle regulation: several Cdks, numerous cyclins and diverse compensatory mechanisms [J]. *Oncogene*, 2009, **28**(33): 2925-2939.

[32] Wiman KG, Zhivotovsky B. Understanding cell cycle and cell death regulation provides novel weapons against human diseases [J]. *J Intern Med*, 2017, **281**: 483-495.

[33] Massagué J. G1 cell-cycle control and cancer [J]. *Nature*, 2004, **432**(7015): 298-306.

[34] Bertoli C, Skotheim JM, de Bruin RA. Control of cell cycle transcription during G1 and S phases [J]. *Nat Rev Mol Cell Biol*, 2013, **14**(8): 518-528.

[35] Tateiwa D, Yoshikawa H, Kaito T. Cartilage and bone destruction in arthritis: pathogenesis and treatment strategy: a literature review [J]. *Cells*, 2019, **8**: 818.

[36] Nagata S. Apoptosis and Clearance of Apoptotic Cells [J]. *Annu Rev Cell Dev Biol*, 2018, **36**: 489-517.

[37] Budihardjo I, Oliver H, Lutter M, *et al*. Biochemical pathways of caspase activation during apoptosis [J]. *Annu Rev Cell Dev Biol*, 1999, **15**: 269-290.

[38] Ma JD, Jing J, Wang JW, *et al*. A novel function of artesunate on inhibiting migration and invasion of fibroblast-like synoviocytes from rheumatoid arthritis patients [J]. *Arthritis Res Ther*, 2019, **21**: 153.

[39] Korb-Pap A, Bertrand J, Sherwood J, *et al*. Stable activation of fibroblasts in rheumatic arthritis-causes and consequences [J]. *Rheumatology (Oxford)*, 2016, **55**: ii64-ii67.

[40] Falconer J, Murphy AN, Young SP, *et al*. Synovial cell metabolism and chronic inflammation in rheumatoid arthritis [J]. *Arthritis Rheumatol*, 2018, **70**: 984-999.

[41] Zhang Q, Peng W, Wei S, *et al*. Guizhi-Shaoyao-Zhimu decoc-

tion possesses anti-arthritic effects on type II collagen-induced arthritis in rats via suppression of inflammatory reactions, inhibition of invasion & migration and induction of apoptosis in synovial fibroblasts [J]. *Biomed Pharmacother*, 2019, **118**: 109367.
[42] Tolboom TC, Pieterman E, van der Laan WH, *et al*. Invasive properties of fibroblast-like synoviocytes: correlation with growth characteristics and expression of MMP-1, MMP-3, and MMP-10 [J]. *Ann Rheum Dis*, 2002, **61**: 975-980.
[43] Weyand CM, Goronzy JJ. Immunometabolism in early and late stages of rheumatoid arthritis [J]. *Nat Rev Rheumatol*, 2017, **13**: 291-301.
[44] Pap T, Meinecke I, Müller-Ladner U. Are fibroblasts involved in joint destruction [J]. *Ann Rheum Dis*, 2005, **64**: iv52-iv54.
[45] Du T, Yan Z, Zhu S, *et al*. QKI deficiency leads to osteoporosis by promoting RANKL-induced osteoclastogenesis and disrupting bone metabolism [J]. *Cell Death Dis*, 2020, **11**(4): 330.
[46] Chen X, Zheng X, Zhang M, *et al*. Nuciferine alleviates LPS-induced mastitis in mice via suppressing the TLR4-NF-κB signaling pathway [J]. *Inflamm Res*, 2018, **67**: 903-911.
[47] McNamee K, Williams R, Seed M. Animal models of rheumatoid arthritis: How informative are they [J]. *Eur J Pharmacol*, 2015, **759**: 278-286.
[48] Chen Z, Bozec A, Ramming A, *et al*. Anti-inflammatory and immune-regulatory cytokines in rheumatoid arthritis [J]. *Nat Rev Rheumatol*, 2019, **15**: 9-17.
[49] Li XF, Sun YY, Bao J, *et al*. Functional role of PPAR-γ on the proliferation and migration of fibroblast-like synoviocytes in rheumatoid arthritis [J]. *Sci Rep*, 2017, **7**: 12671.
[50] Kim EY, Moudgil KD. Immunomodulation of autoimmune arthritis by pro-inflammatory cytokines [J]. *Cytokine*, 2017, **98**: 87-96.
[51] Roberts CA, Dickinson AK, Taams LS. The Interplay Between Monocytes/Macrophages and CD4(+) T Cell Subsets in Rheumatoid Arthritis [J]. *Front Immunol*, 2015, **6**: 571.
[52] Takeuchi Y, Hirota K, Sakaguchi S. Impaired T cell receptor signaling and development of T cell-mediated autoimmune arthritis [J]. *Immunol Rev*, 2020, **294**: 164-176.
[53] Yang Y, Zhang X, Xu M, *et al*. Quercetin attenuates collagen-induced arthritis by restoration of Th17/Treg balance and activation of heme oxygenase 1-mediated anti-inflammatory effect [J]. *Int Immunopharmacol*, 2018, **54**: 153-162.
[54] K. Nistala, L. R. Nistala, L. R. Wedderburn, Th17 and regulatory T cells: rebalancing pro- and anti-inflammatory forces in autoimmune arthritis [J]. *Rheumatology (Oxford)*, 2009, **48**: 602-606.
[55] Heo YJ, Joo YB, Oh H J, *et al*. IL-10 suppresses Th17 cells and promotes regulatory T cells in the CD4 + T cell population of rheumatoid arthritis patients [J]. *Immunol Lett*, 2010, **127**: 150-156.

Cite this article as: WANG Hao, GENG Xiaolong, AI Fangbin, YU Zhilun, ZHANG Yan, ZHANG Beibei, LV Cheng, GAO Ruiyang, YUE Bei, DOU Wei. Nuciferine alleviates collagen-induced arthritic in rats by inhibiting the proliferation and invasion of human arthritis-derived fibroblast-like synoviocytes and rectifying Th17/Treg imbalance [J]. *Chin J Nat Med*, 2024, **22**(4): 341-355.